PROCEEDINGS OF SPIE

SPIEDigitalLibrary.org/conference-proceedings-of-spie

# Design and pre-development of an airborne multi-species differential absorption Lidar system for water vapor and HDO isotope, carbon dioxide, and methane observation

Dherbecourt, J. B., Raybaut, M., Melkonian, J. M., Hamperl, J., Santagata, R., et al.

J. B. Dherbecourt, M. Raybaut, J. M. Melkonian, J. Hamperl, R. Santagata, M. Dalin, V. Lebat, A. Godard, C. Flamant, J. Totems, P. Chazette, V. Pasiskevicius, D. Heinecke, H. Schäfer, M. Strotkamp, J. F. Geus, S. Rapp, H. Sodemann, H. C. Steen-Larsen, "Design and pre-development of an airborne multi-species differential absorption Lidar system for water vapor and HDO isotope, carbon dioxide, and methane observation," Proc. SPIE 11852, International Conference on Space Optics — ICSO 2020, 118521U (11 June 2021); doi: 10.1117/12.2599326

SPIE.

Event: International Conference on Space Optics — ICSO 2021, 2021, Online Only

**International Conference on Space Optics—ICSO 2020**

Virtual Conference

30 March–2 April 2021

*Edited by Bruno Cugny, Zoran Sodnik, and Nikos Karafolas*

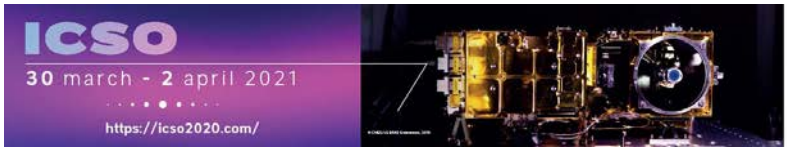



# *Design and pre-development of an airborne multi-species differential absorption Lidar system for water vapor and HDO isotope, carbon dioxide, and methane observation*


International Conference on Space Optics — ICSO 2020, edited by Bruno Cugny, Zoran Sodnik, Nikos Karafolas, Proc. of SPIE Vol. 11852, 118521U · © 2021 ESA and CNES
CCC code: 0277-786X/21/$21 · doi: 10.1117/12.2599326

# Design and pre-development of an airborne multi-species differential absorption Lidar system for water vapor and HDO isotope, carbon dioxide and methane observation

J.B. Dherbecourt*[a], M. Raybaut[a], J.M. Melkonian[a], J. Hamperl[a], R. Santagata[a], M. Dalin[a], V. Lebat[a], A. Godard[a], C. Flamant[b], J. Totems[c], P. Chazette[c], V. Pasiskevicius[d], D. Heinecke[e], H. Schäfer[f], M. Strotkamp[f], J.F. Geus[f], S. Rapp[g], H. Sodemann[h], H.C. Steen-Larsen[h]

[a] DPHY, ONERA, Université ParisSaclay, F-91123 Palaiseau France; [b] Laboratoire Atmosphères Milieux et Observations Spatiales (LATMOS), UMR 8190, CNRS-SU-UVSQ, Paris, France; [c] Laboratoire des Sciences du Climat et de l'Environnement (LSCE), UMR 1572, CEA-CNRS-UVSQ, Gif-sur-Yvette, France; [d] Department of Applied Physics, Royal Institute of Technology (KTH), Roslagstullsbacken 21, 10691 Stockholm, Sweden; [e] SpaceTech GmbH, Seelbachstr. 13, 88090 Immenstaad, Germany; [f] Fraunhofer Institute for Laser Technology, Steinbachstr. 15, 52074 Aachen, Germany; [g] InnoLas Laser GmbH, Justus-von-Liebig- Ring 8, 82152 Krailling, Germany; [h] Geophysical Institute, University of Bergen and Bjerknes Centre for Climate Research, Bergen, Norway

*jean-baptiste.dherbecourt@onera.fr

## ABSTRACT

We report on the current design and preliminary developments of the airborne Lidar Emitter and Multi-species greenhouse gases Observation iNstrument (LEMON), which is aiming at probing $H_2O$ and its isotope HDO at 1982 nm, $CO_2$ at 2051 nm, and potentially $CH_4$ at 2290 nm, with the Differential Absorption Lidar method (DIAL). The infrared emitter is based on the combination of two Nested Cavity OPOs (NesCOPOs) with a single optical parametric amplifier (OPA) line for high-energy pulse generation. This configuration is enabled by the use of high-aperture periodically poled KTP crystals (PPKTP), which provide efficient amplification in the spectral range of interest around 2 µm with slight temperature adjustments. The parametric stages are pumped with a Nd:YAG laser providing 200 mJ nanosecond double pulses at 75 Hz. According to parametric conversion simulations supported by current laboratory experiments, output energies in the 40 - 50 mJ range are expected in the extracted signal beam whilst maintaining a good beam quality ($M^2 < 2$). The ruler for all the optical frequencies involved in the system is planned to be provided by a GPS referenced frequency comb with large mode spacing (1 GHz) against which the emitter output pulses can be heterodyned. The frequency precision measurement is expected to be better than 200 kHz for the optical frequencies of interest. The presentation will give an overview of the key elements of design and of preliminary experimental characterizations of sub-systems building blocks.

**Keywords:** Lidar, Parametric Sources, Greenhouse Gases

## 1. INTRODUCTION

Differential Absorption Lidars (DIAL) and Integrated Path Differential Absorption Lidars (IPDA) for remote sensing of atmospheric gas components such as water vapor, carbon dioxide, and methane are being developed by several research institutes and national agencies in order to bring advanced capabilities to the observation of water and carbon cycles, be that from ground-based, airborne, or spaceborne platforms[1-13]. Although the possibility to measure greenhouse gases from space with active Lidar methods is expected to come with significant benefits such as measurement independency from solar illumination[1,2,5], the technical and scientific challenges for this kind of mission are highly demanding. As a consequence, ongoing efforts to leverage the readiness level of critical technologies such as high-energy infrared laser sources and their evaluation by airborne test campaigns are still important steps forward on the path for these future missions. In this paper we give an overview of the system layout design and of the foreseen technical realizations for a

multispecies DIAL instrument that is intended to demonstrate airborne operation as well as few key performances such as emitter output power and frequency stability in line with space-borne instrumentation requirements. These technical developments are being carried out in the frame of the EU H2020 LEMON project[14] in collaboration with atmosphere and climate research laboratories in order to orientate and extend scientific opportunities for this instrumentation. In this particular regard, one driving objective beyond airborne demonstration is to propose a set-up that could provide vertical DIAL measurement of water vapor and its isotope HDO, in order to improve the current range-resolved observation capabilities for these molecules in the atmosphere and our representation of the water vapor cycles[15]. As is illustrated in the following parts, this particular type of measurement is essentially made possible in the 2 µm spectral window, where the water vapor main isotope and HDO display separated absorption lines with adequate differential optical depth for kilometric ranges.

## 2. BACKGROUND

The main technological component at the core of the LEMON instrument is the NesCOPO-based MOPA (Master oscillator Power Amplifier) emitter architecture that has been developed at ONERA for several years and applied to a variety of different spectral ranges for remote sensing application purposes[16]. This architecture has been suggested as a generic and versatile injection-seeding-free tunable parametric source, that might benefit from the heritage of current space Lidar missions, relying on parametric conversion of high-power 1 µm pump laser such as Aeolus, Earthcare, and Merlin[17,18]. The NesCOPO architecture relies on doubly resonant Optical Parametric Oscillation (OPO) within slightly dissociated signal and idler optical cavities. With sufficiently narrow single-frequency pump laser, along with proper cavity length dissociation and emission bandwidth tailoring, a single pair of signal and idler modes can be selected and tuned at the output of the cavities by Vernier spectral filtering (see reference 16 for more details on the geometry and design principles).

In the nanosecond regime, and in combination with high power OPAs, the extracted signal and idler can be brought to high energy levels (several 10 mJ) that are compliant with Lidar applications as already demonstrated in previous work[13]. More recently, first steps of maturation of this architecture have been tackled in an attempt to come with high intrinsic stability properties for the NesCOPO-based MOPA in terms of frequency, power, and beam pointing drifts. Indeed, one important challenge with the doubly resonant configuration is its sensitivity to external fluctuations such as nonlinear crystal temperature or pump beam pointing, which might result in frequency drift and mode hopping. Active control and correction can be applied thanks to piezoelectric transducers mounted on the OPO external cavity mirrors, but anticipative special care has to be brought in order to start from high intrinsic stability levels.

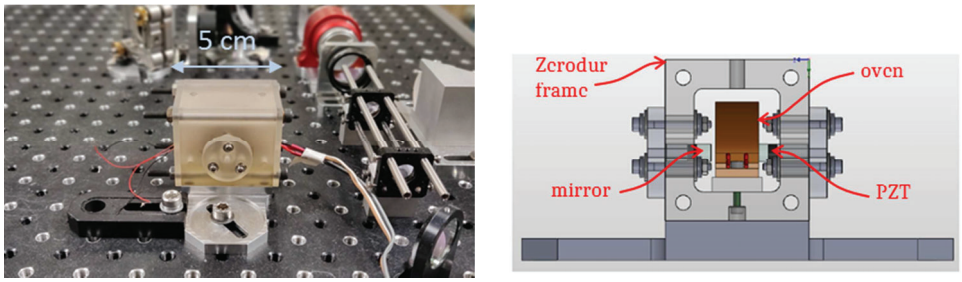


*(a)* *(b)*

Figure 1. NesCOPO assembly within a Monobloc zerodur frame as developed during ESA TRP GENUIN (OPA stages not visible in the picture) *(a)*. CAD view from the side *(b)*.

To this end, a ruggedized opto-mechanic assembly built around a low expansion glass frame (Figure 1*(a) & (b)*) with stringent mechanical alignment tolerances has been proposed and realized within an ESA TRP project (GENUIN). The NesCOPO cavity temperature is controlled with a copper oven in which the nonlinear material is located (Periodically Lithium Niobate PPLN). In combination with state-of-the-art OPA stages based on high-aperture PPKTP[19] nonlinear crystals (Figure 1 *(c)*), up to 11 mJ at 2051 nm wavelength suitable for $CO_2$ sensing from space have been extracted for 60 mJ of initial pump energy at 1 µm. In free-running operation, mode hopping happens within a 30 min to 1 h time period, which is attributed to residual cavity length or pump wavelength drifts. In between mode hopping phases, the free-running central frequency drifts by a few MHz (2 MHz Allan deviation @ 10 s integration time), and the output energy standard deviation is smaller than 2 % over 1 min as illustrated in Figure 2*(b)*.

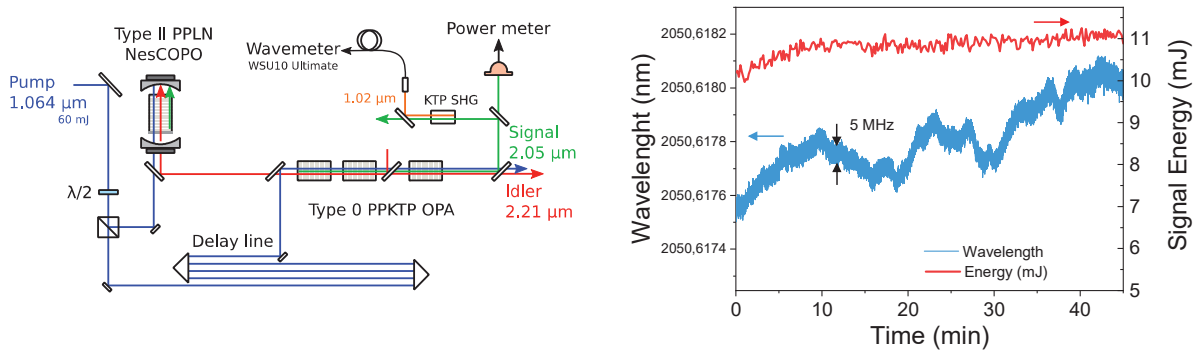


*(a)* *(b)*

Figure 2. Scheme of the NesCOPO-based MOPA emitter *(a)*. Free-running central frequency and power drifts recorded at the output of the OPA stages *(b)*. The wavelength is recorded pulse to pulse with a WSU10 High Finesse wavelength-meter, and the energy is directly measured with a joule-meter on the extracted signal beam working around 2051 nm in the vicinity of the R30 $CO_2$ absorption line. The amplification is provided by 3 cascaded high-aperture 5x5 mm² PPKTP crystals pumped with 60 mJ 10 ns pulses at 1064 nm (30 Hz repetition rate).

## 3. SPECTRAL WINDOWS

The general goal in the design is to build around this technological block and MOPA arrangement in order to address the main objectives of the LEMON project which can be summarized as *i)* providing multiple-species probing capability, *ii)* demonstrating key performances for space application, and *iii)* achieving airborne operation and measurement campaigns.

For these purposes the 2 µm spectral range is well adapted as it contains several absorption lines for the molecules of interest with differential optical depth (DOD) levels suitable in various ranges of applications from ground-based to spaceborne measurement scenarios. In particular the spectral window around 2051 nm is well suited for $CO_2$ probing with the R30 absorption line, which is well adapted for IPDA measurement from space[3, 4]. This spectral window might also be used to complementary probe water vapor, which has been suggested for example by NASA[6]. Besides $CO_2$ probing, another original spectral window located around 1982 nm is targeted to provide HDO isotopic ratio measurement (Figure 3*(b)*), since HDO and $H_2O$ main isotope provide well separated and comparable absorption lines in terms of optical depth.

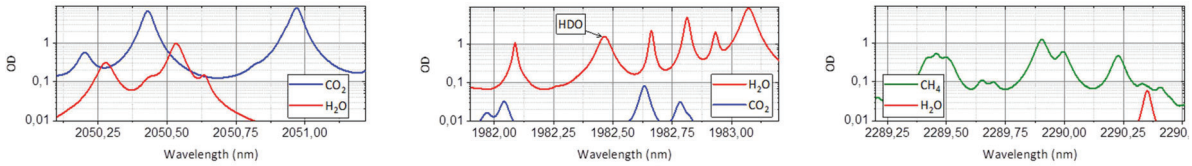


*(a)* *(b)* *(c)*

Figure 3. Optical depth calculated within the three main spectral windows of interest with HITRAN 2016 for a 6 km two-way vertical path (from ground). $CO_2$ window *(a),* water vapor and HDO window *(b)*, $CH_4$ window *(c)*.

Finally, the 2290 nm window has also been suggested for $CH_4$ probing from space[3], with well-adapted DOD and low interference from other molecules. The 2290 nm window is also interesting from the instrumental point of view as it is the natural complementary window for the idler wave in an OPO pumped at 1064 nm and tuned for signal emission in the 1982 nm spectral window. From space application perspective, these spectral windows are however more prospective than the 2051 nm one for $CO_2$ measurement, since the spectroscopy is not as well established, and also isotopic ratio measurement scenarios require the emission of at least three wavelengths.

# 4. INSTRUMENT DESIGN AND ARCHITECTURE

The overall architecture is the combination of different technologies which have been proposed and designed in order to keep the instrumental approach as generic as possible. As for all DIAL instrumentation, the main technological building blocks are composed of *i)* a transmitter unit, which generates the laser beams with the proper energies and spectro-temporal characteristics, *ii)* a frequency reference unit, which ensures accurate knowledge of the emitted wavelengths, *iii)* a receiver module composed of a high-aperture telescope, low-noise detector, and digitizer to record the signals.

## 4.1 Emitter architecture

In the LEMON design, the infrared emitter is based on the combination of two NesCOPOs with a single optical parametric amplifier line optimized for high-energy pulse extraction in the signal beam as illustrated in Figure 4. The two-OPOs configuration was chosen in order to work at a fixed thermo-mechanical point and reduce the risks of misalignment or beam quality degradation that might occur with temperature or mechanical tuning. The OPOs are based on periodically poled Lithium Niobate (PPLN) nonlinear crystals. In the first NesCOPO, the quasi-phase matching (QPM) condition is tuned to get the emitted signal in the 1982 nm window suitable for water vapor and HDO isotopic ratio sounding. As mentioned earlier, the idler wave is generated in the 2290 nm window suitable for $CH_4$. The second NesCOPO QPM condition is tuned for signal emission in the $CO_2$ 2051 nm window. The idler beams are ~~out~~ coupled out and combined with dichroic mirrors in order to be sent in the OPA line. For these NesCOPOs, working around 2 µm, the typical extracted idler energy is ranging in the ~20 µJ. As a consequence, reaching several tens of mJ at the OPA stages output corresponds to a significant gain level~~s~~ requirement superior to 30 dB.

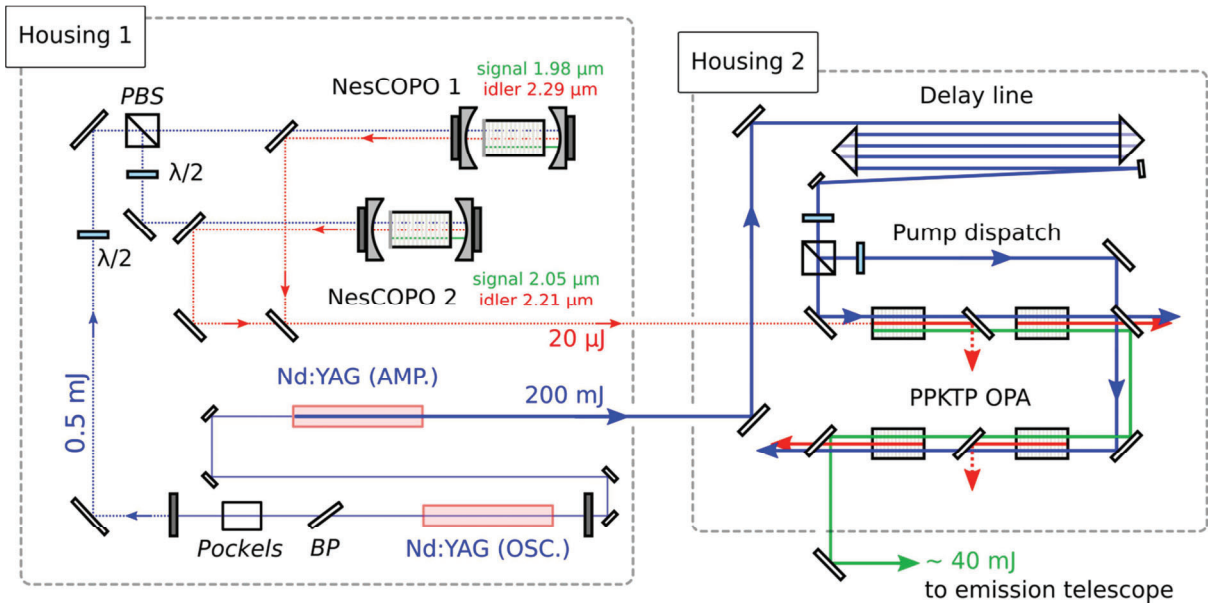


Figure 4. Simplified optical layout of the emitter. (PBS) stands for polarizing beam splitter, (λ/2) for half-wave plate, and (BP) for Brewster plate.

The OPA line is composed of cascaded Rb:PPKTP nonlinear crystals with high transverse aperture of 5 x 5 mm². QPM in PPKTP crystals enables to reach a significantly higher effective nonlinear coefficient of 9.3 pm/V, compared to the typical 2.5 pm/V obtainable in conventional bulk KTP phase matched through bi-refringence, while still enabling high energy conversion thanks to the high aperture and damage threshold (in the 1 -10 J/cm² range). The poling has been produced with a 38.75 µm period by using lithography and pulsed electric field poling procedure[19]. The calculated gain spectra for 10 mm long PPKTP are shown in Figure 5*(a)*, and reveal the possibility to address all the targeted spectral windows provided slight temperature adjustment of 25 °C.

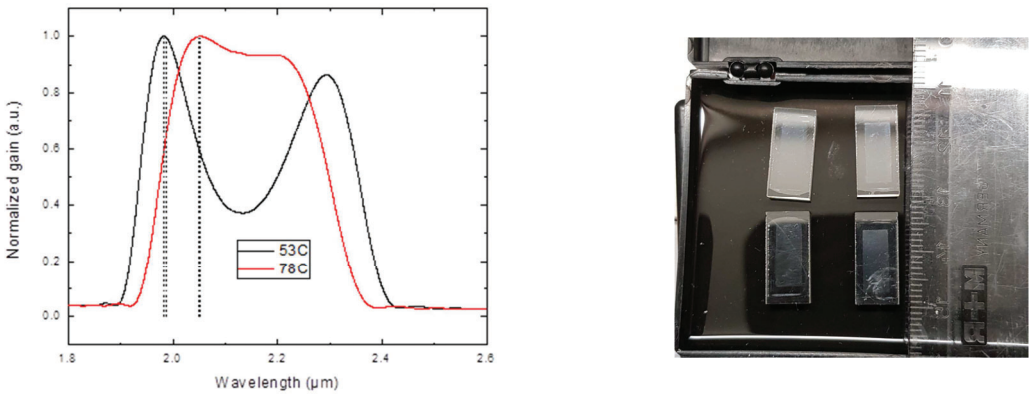


*(a)* *(b)*

Figure 5. PPKTP OPA gain bandwidth calculated for 10 mm long crystals and different temperature with a 38.75 µm poling period. The dotted lines designate target spectral ranges for the signal waves (a). Picture of 4 PPKTP crystals (b).

The design strategy for these OPA stages was to optimize the output energy in the signal waves in the 1982 nm and 2051 nm windows, while keeping a reasonably good expected beam quality (typically $M^2 < 1.5$) in a compact set-up. For this purpose, the adjustable parameters are the number of crystals and their length, the pump power distribution in the different stages, and the potential filtering of the idler wave between the different stages. The choice was made to keep the same beam diameter size of 2.9 mm diameter, determined by the aperture of the OPA crystals, in all stages in order to significantly reduce the footprint of the pump distribution stages by limiting the number of beam shaping telescopes and combiner components, and also to limit the laser-induced damage risks by maintaining a mean fluence lower than 2.5 J/cm². The optimization of the different free parameters was carried out with a proprietary simulation tool from ILT (OPT)[20] and converged to a design consisting of two stages, with two 12 mm long crystals in stage 1 and one 12 mm long and one 6 mm long crystal in stage 2. Signal extraction and beam quality optimization is achieved by idler beam filtering in between all crystals as illustrated Figure 4. Idler removal is an efficient way to reduce saturation and back-conversion effects in the OPA. Figure 6 illustrates pump distribution optimization in the two stages. Increasing pump energy in the first stage with the highest gain is beneficial for the overall extracted power, with a tradeoff on the beam quality which significantly degrades for extracted energies over 50 mJ. In order to remain in a comfortable spot in terms of beam quality, pump distribution in the first stage is chosen within a range where the expected $M^2$ does not exceed 1.3, which would set the expected extracted signal energy in the 40–50 mJ range. As illustrated in Figure 6 and considering a total of 200 mJ pump energy, this would lead to an almost balanced energy distribution in the two OPA stages which is also an interesting tradeoff in regards of laser-induced damage since fluence will be spread evenly in the crystals.

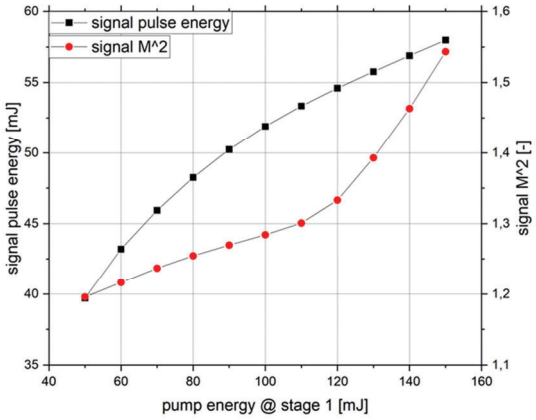


Figure 6. Extracted signal beam energy and $M^2$ calculated at the output of the OPA line as a function of pump energy in the first OPA stage. The configuration is composed of two stages with two PPKTP crystals in each stage and idler filtering. The total pump energy distributed in the OPA line (stage 1+2) is 200 mJ.

### 4.2 Emitter Layout

The overall emitter layout is exposed hereafter in Figure 7 with the housings containing the pump laser, the OPOs, and the OPA sub-systems. In the first housing, the pump laser is built by InnoLas in a MOPA configuration. The pump radiation is generated from a folded oscillator to produce 15 ns pulses, which is a favorable regime for the OPO/OPA stages. It is injection seeded for single-frequency operation, and further amplified in a second Nd:YAG rod to reach 200 mJ energy pulses at a repetition rate of 150 Hz. A specific pumping timing is applied to operate in double-pulse mode (i.e. 75 Hz double-pulse emission) with a 500 µs delay. The NesCOPOs are located in the same housing as close as possible to the laser oscillator in order to minimize pump beam pointing fluctuations. Thanks to their low oscillation threshold, the OPOs are pumped directly with a ~ 0.5 mJ leakage beam from the rear laser cavity mirror. The OPA stages and delay line are built following a similar approach within a monolithic aluminum housing. The emitter is then mounted on a carbon 'meta-bench', which also hosts the beam shaping and steering components for the lidar emission, as well as an integrating sphere for energy monitoring. This carbon meta-bench is designed to be connected at the bottom to the receiver as illustrated in Figure 7.

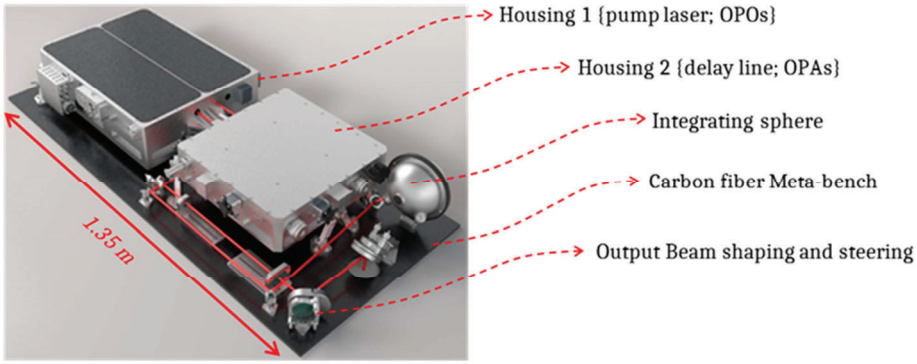


Figure 7. Overall emitter layout on meta-bench frame together with emission beam shaping and energy calibration systems.

Specific care has been brought to the thermo-mechanical management of the housings in order to withstand the expected aircraft environment (ATR 42 platform from the SAFIRE fleet). The design, supported by FEM simulation of thermal deformations and vibrational modes, is based on isostatic mounting of the housings arranged in a way to reduce displacements due to temperature change and essentially allow movements along the beam transfer direction between the two housings to limit pointing fluctuations.

### 4.3 Frequency reference unit

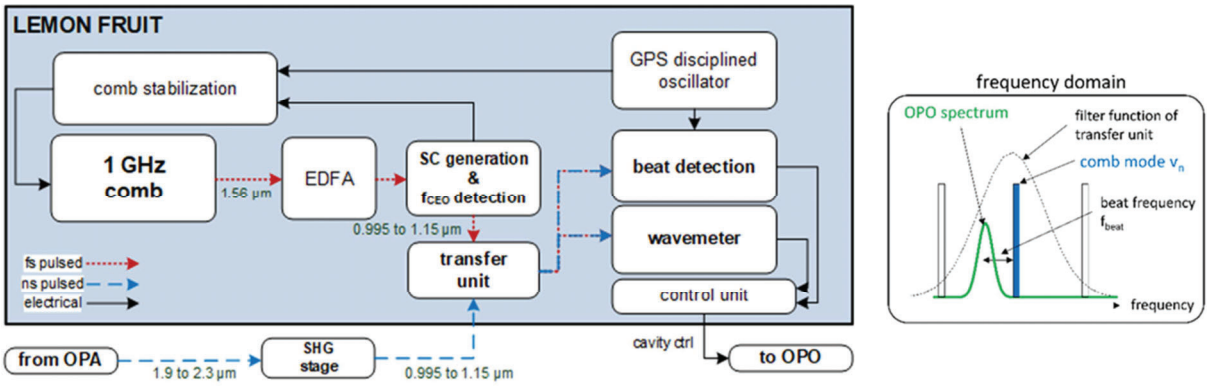


*(a)* *(b)*

Figure 8. LEMON Frequency Reference UnIt (FRUIT) principle diagram (a). Beat note measurement principle (b). EDFA is Erbium Doped Fiber Amplifier, SC stands for Super Continuum, and SHG for Second Harmonic Generation.

Gas concentration measurement from space requires high-accuracy frequency measurement of the online and offline pulses. For this purpose, the approach followed for the LEMON instrumentation consists in using a referenced frequency comb and beat note analysis in order to retrieve this frequency value. A more detailed overview of this approach and of the current technological development carried out at SpaceTech is proposed in a separate presentation (ICSO 2020 poster session n° P093). The general principle is described in the diagram of Figure 8. The key design component is the generation of supercontinuum radiation expanding in the 0.995 µm – 1.15 µm region starting from a 1.56 µm femtosecond laser, which enables carrier envelop frequency offset stabilization of the comb through f-2f interferometry as well as optical frequency measurement through beat note analysis between a comb line and the emitter pulses. To perform this heterodyning, a leak from the OPA stages is extracted for second harmonic generation (SHG) in order to match the spectral range of the supercontinuum. In the current architecture direct beat note analysis between the SHG radiation and a single comb mode is investigated in order to skip the use of additional CW transfer laser sources. For this purpose an auxiliary low resolution wavemeter is employed in order to identify the index of the comb mode involved in the beating.

### 4.4 Receiver design

As for the emitter part, the general design approach for the receiver is based on a trade-off between airborne operation demonstrations while keeping the capacity to use the system in range-resolved DIAL configuration, which is a key feature especially for water vapor measurement scenarii. In order to be able to retrieve range-resolved signals, the telescope will be a 35 cm diameter Newton telescope provided by SkyVision, with a focal length of 1250 mm. Fiber coupling is envisioned, in order to separate the detection rack from the main instrument, with an expected field of view of 700 µrad. The detector will be a commercial thermoelectrically cooled extended InGaAs PIN photodiode with peak sensitivity at 2 µm, integrated with custom amplifier and digitizer. The detection block is shown in Figure 9 *(c)*. The PIN, the amplifier and a 16 bits digitizer are mounted on the same card and linked to a FPGA in order to preprocess the numerical signals before data recording. The noise-equivalent power of the detection chain is 0.6 pW/√Hz, for a 1.8 MHz bandwidth.

## 5. INTEGRATION FOR AIRBORNE OPERATION

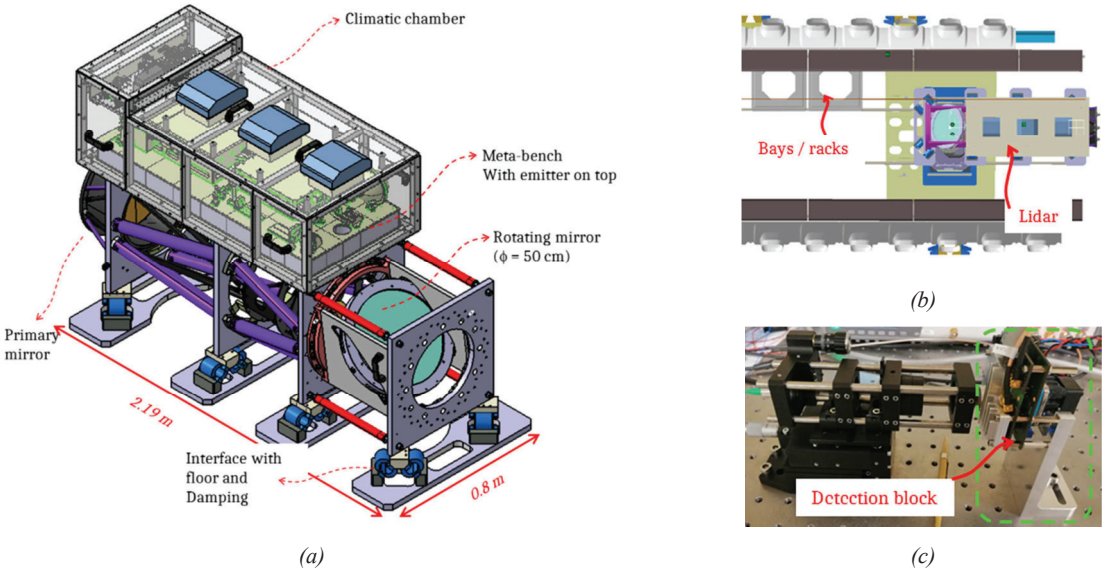


*(a)* *(b)* *(c)*

Figure 9. LEMON instrument (a). Preview of the instrument implementation within the aircraft cabin (b). Thermo-electrically cooled InGaAs photodiode assembly with transimpedance amplifier and integrated digitizer (c).

The instrument will be integrated within the Safire ATR42 science aircraft, which offers two windows for zenith or nadir line of sights. In order to be able to perform horizontal, zenith (for ground-based measurements or alignment verifications within the aircraft) or nadir measurements, a rotative plane mirror is placed at the output of the lidar, (Figure 9). In order to sustain the vibration environment, special care is taken on the isolation between the aircraft and

the instrument: vibration damping solutions are currently being tested. Moreover, a thermally controlled box has been designed to regulate the temperature around the emitter (Figure 9 *(a)*).

## CONCLUSION

We aim at developing a DIAL instrument with the goals of both airborne demonstration and range-resolved measurement from the ground to provide vertical DIAL retrievals of water vapor and its isotope HDO in the 1982 nm spectral region, and carbon dioxide around 2051 nm. To be able to achieve such goals, an adapted OPO/OPA-based emitter architecture, including a specific frequency reference unit based on beat note analysis with a frequency comb, is currently being built. Special care was also taken with respect to the overall instrument design in order to sustain the environment of the ATR42 aircraft. Future work will be dedicated to the emitter realization and characterization, its integration within the overall DIAL system, ground-based testing, and future airborne campaigns.

## ACKNOWLEDGEMENTS

This research has received funding from the European Union's Horizon 2020 research and innovation program under grant agreement N° 821868, and from French National research Agency ANR under grant N° ANR-16-CE01-0009.

## REFERENCES

[1] ESA, "Report for Assessment, SP-1313/1," A-SCOPE - Advanced space carbon and climate observation of planet earth, ESA-ESTEC, Noordwijk, The Netherlands (2008).
[2] ASCENDS Workshop Steering Committee, Active Sensing of CO2 Emissions over Nights, Days, and Seasons (ASCENDS) Mission NASA Science Definition and Planning Workshop Report (2008).
[3] G. Ehret, C. Kiemle, M. Wirth, A. Amediek, A. Fix, and S. Houweling, "Space-borne remote sensing of CO2, CH4, and N2O by integrated path differential absorption lidar: a sensitivity analysis," Appl. Phys. B **90**, 593–608 (2008).
[4] Jérôme Caron and Yannig Durand, "Operating wavelengths optimization for a spaceborne lidar measuring atmospheric $CO_2$," Appl. Opt. **48**, 5413-5422 (2009).
[5] Ehret, G.; Bousquet, P.; Pierangelo, C.; Alpers, M.; Millet, B.; Abshire, J.B.; Bovensmann, H.; Burrows, J.P.; Chevallier, F.; Ciais, P.; Crevoisier, C.; Fix, A.; Flamant, P.; Frankenberg, C.; Gibert, F.; Heim, B.; Heimann, M.; Houweling, S.; Hubberten, H.W.; Jöckel, P.; Law, K.; Löw, A.; Marshall, J.; Agusti-Panareda, A.; Payan, S.; Prigent, C.; Rairoux, P.; Sachs, T.; Scholze, M.; Wirth, M. MERLIN: A French-German Space Lidar Mission Dedicated to Atmospheric Methane. Remote Sens. 2017, 9, 1052.
[6] U. N. Singh, M. Petros, T. F. Refaat, J. Yu, S. Ismail, "Column carbon dioxide and water vapor measurements by an airborne triple-pulse integrated path differential absorption lidar – novel lidar technologies and techniques with path to space," Proc. SPIE 10562, International Conference on Space Optics — ICSO 2016, 105621R (25 September 2017)
[7] G. Wagner and D. Plusquellic, "Ground-based, integrated path differential absorption LIDAR measurement of CO2, CH4, and H2O near 1.6 μm," Appl. Opt. **55**, 6292 (2016).
[8] J. B. Abshire, H. Riris, C. J. Weaver, J. Mao, G. R. Allan, W. E. Hasselbrack, and E. V. Browell, "Airborne measurements of CO2 column absorption and range using a pulsed direct-detection integrated path differential absorption lidar," Appl. Opt. **52**, 4446 (2013).
[9] A. Amediek, A. Fix, M. Wirth, and G. Ehret, "Development of an OPO system at 1.57 μm for integrated path DIAL measurement of atmospheric carbon dioxide," Appl. Phys. B **92**, 295–302 (2008).
[10] S. Ishii, K. Mizutani, P. Baron, H. Iwai, R. Oda, T. Itabe, H. Fukuoka, T. Ishikawa, M. Koyama, T. Tanaka, I. Morino, O. Uchino, A. Sato, and K. Asai, "Partial CO 2 Column-Averaged Dry-Air Mixing Ratio from Measurements by Coherent 2- μ m Differential Absorption and Wind Lidar with Laser Frequency Offset Locking," J. Atmos. Ocean. Technol. **29**, 1169–1181 (2012).
[11] S. Kameyama, M. Imaki, Y. Hirano, S. Ueno, S. Kawakami, D. Sakaizawa, and M. Nakajima, "Performance improvement and analysis of a 1.6 μm continuous-wave modulation laser absorption spectrometer system for

CO2 sensing," Appl. Opt. **50**, 1560 (2011).
[12] Fabien Gibert, Jessica Pellegrino, Dimitri Edouart, Claire Cénac, Laurent Lombard, Julien Le Gouët, Thierry Nuns, Alberto Cosentino, Paolo Spano, and Giorgia Di Nepi, "2-µm double-pulse single-frequency Tm:fiber laser pumped Ho:YLF laser for a space-borne CO2 lidar," Appl. Opt. 57, 10370-10379 (2018).
[13] Erwan Cadiou, Dominique Mammez, Jean-Baptiste Dherbecourt, Guillaume Gorju, Jacques Pelon, Jean-Michel Melkonian, Antoine Godard, and Myriam Raybaut, "Atmospheric boundary layer CO2 remote sensing with a direct detection LIDAR instrument based on a widely tunable optical parametric source," Opt. Lett. 42, 4044-4047 (2017)
[14] https://lemon-dial-project.eu/
[15] C. Flamant and D. Bruneau, Simulateur de lidar spatial H2O, CNES R&T report LATMOS-R&T_H2O-RP-04/CNES R-S13/OT-0002-074 (2014)
[16] Godard, A., Raybaut, M. and Lefebvre, M. (2017). Nested Cavity Optical Parametric Oscillators – A Tunable Frequency Synthesizer for Gas Sensing. In Encyclopedia of Analytical Chemistry, R.A. Meyers (Ed.).
[17] Alberto Cosentino, Alessandro D'Ottavi, Paolo Bravetti, Enrico Suetta, "Spaceborne lasers development for ALADIN instrument on board ADM-Aeolus ESA mission," Proc. SPIE 9626, Optical Systems Design 2015: Optical Design and Engineering VI, 96261U (23 September 2015); https://doi.org/10.1117/12.2195981
[18] Sven Hahn, Markus Bode, Jörg Luttmann, Dieter Hoffmann, "FULAS: high energy laser source for future LIDAR applications," Proc. SPIE 11180, International Conference on Space Optics — ICSO 2018, 111805F (12 July 2019); (https://doi.org/10.1117/12.2536114)
[19] A. Zukauskas, N. Thilmann, V. Pasiskevicius, F. Laurell, and C. Canalias “5 mm thick periodically poled Rb-doped KTP for high energy optical parametric frequency conversion” Optical Mat. Express, 1, 201-206 (2011).
[20] Wester, R. (2013). Physical optics methods for laser and nonlinear optics simulations, Advanced Optical Technologies, 2(3), 247-255. doi: https://doi.org/10.1515/aot-2012-0060